J Electroceram (2006) 16: 9–14
DOI 10.1007/s10832-006-0902-1

# Electron beam lithographic techniques and electrochemical reactions for the micro- and nanostructuring of surfaces under extreme conditions

**T. Djenizian · P. Schmuki**

Received: January 7, 2005 / Revised: February 8, 2005 / Accepted: March 11, 2005


**Abstract** An overview of nanostructuring of surfaces using electron-beam lithographic approaches combined with electrochemical techniques is given. We report the compatibility of conventional electron-beam lithography as well as an alternative method (electron-beam-induced deposition) with electroplating of metals and electrochemical etching of the substrates. This paper describes how to exploit these electron beam-writing techniques for highly selective electrochemical reactions at various surfaces. The ability to use electron beam-induced nanomasking even under extreme conditions is highlighted for the fabrication of structures in the sub-100 nm range.

**Keywords** Nanopatterning · Electron-beam lithography · Electron-beam-induced deposition · Electrochemical reactions · Extreme conditions

## 1. Introduction

Due to significant theoretical and technological new advances, nanostructuring of surfaces has attracted the attention of physicists, chemists and biologists. Their continuous demand for shrinking the dimensions of structures to reach the nanometer scale is mainly motivated by the discovery of new behaviors dominated by unique properties of nanomaterials because the nanoscale is not only another step toward miniaturization but it is also a qualitatively new scale. To date, optical lithography is the main technique used for the integrated circuit (IC) industry but the current strategies employed are blocked by optical diffraction. Thus, new approaches have been explored to fabricate structures in the sub-100 nm range—see e.g. reports on LIGA (*Lithographie, galvanoformung und abformung*, the German words for Lithography, Electroplating and Molding process) [1], micro contact printing [2] and proximal probe lithography [3–5].

With several advantages such as a low cost, simplicity, and compatibility with a wide range of micropatterning processes, electrochemistry is strongly emerging in nanotechnologies [6]. Particularly, the ability to combine electrochemical techniques with direct nanopatterning approaches such as electron beam (e-beam) writing is highly valuable to fabricate high aspect ratio structures in the sub-100 nm range. Besides the direct e-beam patterning of electrochemically modified surfaces (see e.g. [7]), we report electrochemical techniques that have been widely used with conventional e-beam lithography (EBL) as well as an alternative e-beam writing approach to produce nanostructures even under extreme conditions.

## 2. Nanostructuring using conventional EBL and electrochemical reactions

### 2.1. EBL technique

EBL followed soon after the development of the scanning electron microscope (SEM) in 1955 [8] and was one of the earliest processes used for IC fabrication dating back to 1957 [9]. As early as 1965, sub-100 nm resolution was reported [10] and was optimized in 1976, with improved electron optics [11]. To date, EBL is widely exploited to produce structures in the sub-100 nm range [12–16]. Compared with photolithography, the lateral resolution achieved by EBL is higher because the beam of electrons can be focused to

T. Djenizian (✉)· P. Schmuki
Institute for Surface Science and Corrosion (LKO), Dept. of Materials Science, Martensstr. 7, D. 91058 Erlangen, Germany
e-mail: Thierry@ww.uni-erlangen.de

produce probe size as small as 1 nm. More over, electrons do not suffer from optical thin-film interference. However, several parameters other than the size of the beam determine the extent of the exposed volume in a layer of an e-beam sensitive materials so-called resist. Depending on the intended applications, the accelerating voltage, the electron scattering as well as the thickness of the resist play a crucial role [17]. For ICs, where at present low beam energy and thick conventional resists are used, electron scattering is the most important factor whereas for nanolithography, which utilizes high beam energy and thin resists, secondary electron emission is the most dominant factor. The resolution of EBL depends also on the chemical nature of the resist. Recently, new class of resists such as organic self-assembled mono layers (SAMs) has been developed to fabricate structures below 10 nm [18, 19]. Except for more recent reports of atomic resolution with a proximal probe (see e.g. [20]), the resolution of EBL has been unsurpassed by any other form of lithography.

However, the technique is far too slow for a mass production and up to now is mainly used to produce masks, rapid prototyping of ICs and specific small volume production [21, 22].

The principle of pattern transfer based on EBL is depicted in Fig. 1. The process steps are essentially the same as those used for photolithography, except that the pattern on the resist is obtained by scanning directly the focused particle beam across the surface (Fig. 1(a)). The lithographic sequence begins with coating substrates with a positive or negative resist. Positive resists such as poly(methyl-methacrylate) (PMMA) become more soluble in a developing solvent after exposure because the radiation causes local bond breakages and thus chain scission. As a result, the exposed regions containing material of lower mean molecular weight are dissolved after development (Fig. 1(b)). By contrast, negative resists become less soluble in solvent after exposure because cross-linking of polymer chains occurs. In this case, if a region of a negative resist-covered film is exposed, only the exposed region will be covered by resist after development. Subsequently, the resist-free parts of the substrate can be selectively coated with metal—as it is shown in Fig. 1(c)—or etched before removal of the unexposed resist leaving the desired patterns at the surface (Fig. 1(d)).

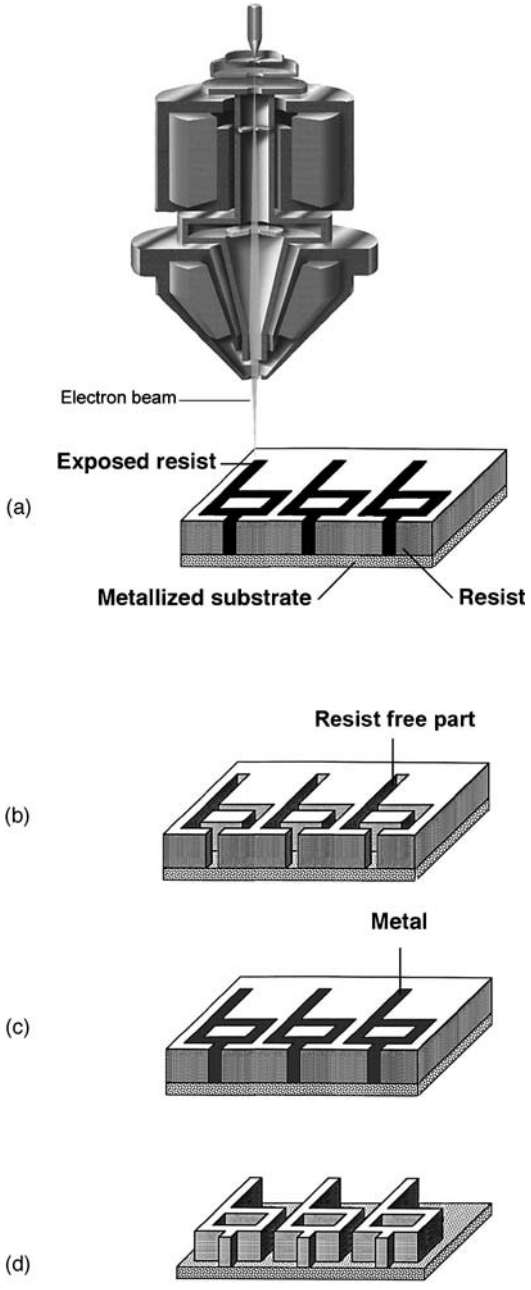


**Fig. 1** Principle of the nanostructuring of surfaces using conventional EBL technique and electroplating, (a) e-beam exposure of a positive resist, (b) removal of the exposed resist, (c) filling of the resist-free locations with metal using electroplating technique, and (d) removal of the unexposed resist leaving high aspect ratio metallic nanostructures at the surface

## 2.2. Nanostructuring by EBL and electroplating

Fabrication of metallic nanostructures has been widely explored using conventional EBL and lift off techniques. However, this top-down approach cannot be used for the fabrication of high aspect ratio vertical structures since gradual accumulation of materials at the top of the resist blocks and closes the opening of the structures during the evaporation of metal. Electroplating of metals into the holes formed in PMMA resist is a convenient alternative to circumvent this problem [23]. For example, the fabrication of dense ultra-small magnetic arrays by filling nanoholes with electroplated Ni has been reported [24]. Electrodeposition of Ni was performed from Ni sulfonate electrolyte by potentiostatic experiments. Depending on the electroplating time, high aspect ratio Ni pillars or mushroom-like structures were

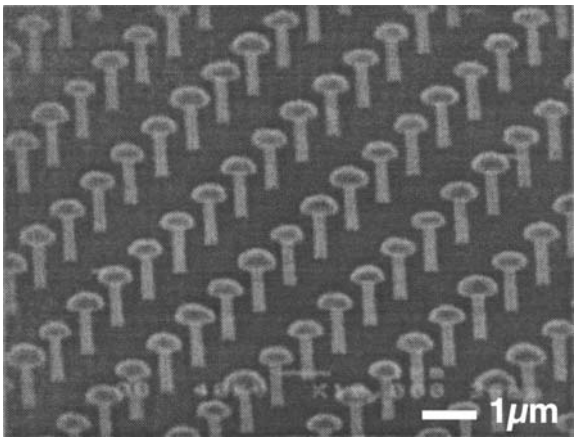


**Fig. 2** SEM micrograph of an overplated micromagnet array showing the mushroom shape characteristic of isotropic metal deposition

obtained. Figure 2 shows a SEM micrograph of mushroom shape micromagnetic arrays grown by overplating after removal of PMMA by oxygen plasma etching. This bottom-up approach has been also used to produce arrays of 30 nm magnets with 80 nm pitch (distance between two magnets). From a practical use point of view, this packing density translates into an equivalent memory storage capacity of over Gbit/in$^2$. The density of the magnetic arrays can be further increased by optimizing the EBL parameters. Under optimal conditions, the formation of 12 nm holes in 100 nm thick PMMA resist with spacing of 45 nm have been reported showing the high resolution achieved by EBL and electrodeposition of metals [24].

### 2.3. Nanostructuring by EBL and Electrochemical Etching

A similar approach has been used for the formation of monocrystalline pore arrays in anodic alumina [25]. For this, the pattern of hexagonal pattern squires was written on the PMMA resist hole by hole with EBL. After removal of the irradiated parts, the pattern was transferred to the Al substrate by using a wet chemical etch in phosphoric and nitric acids. Then, PMMA was removed and the Al substrate was finally anodized in an oxalic acid solution under constant voltage. When the pore distance, which depends on the anodic voltage, matches the prepattern pitches well, the pattern can act as initiation points and guide the pore growth in the anodic film. Figure 3 shows a SEM micrograph of an ordered pore array prepared with 200 nm interpore distance. In this case, the anodic voltage was adjusted to 85 V based on the relationship between the pore distance and the anodic voltage. Under these conditions, very high aspect ratios (around 500) could be achieved.

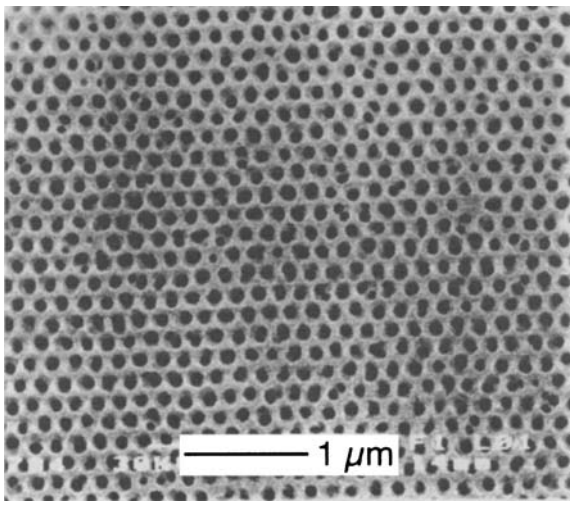


**Fig. 3** Monocrystalline pore arrays in ordered porous alumina prepared with prepattern guided anodization. The prepattern with a pitch of 200 nm was induced by using EBL. Anodization was conducted in 0.04 oxalic acid at 5°C at 85 V, and pores were widened in 5 wt.% phosphoric acid at 20°C for 30 min. Reproduced by permission of the Electrochemical society, Inc

## 3. Micro- and nanostructuring using e-beam-induced carbonaceous deposition (EBICD) approach and electrochemical reactions

### 3.1. E-beam-induced deposition (EBID) technique

EBID is a single-step and direct-writing technique using the beam of electrons to grow 3D nanostructures. The principle is based on the e-beam-induced decomposition of adsorbed precursor molecules present in the chamber of the e-beam instrument resulting in a solid deposit at the point of impact of the beam. When organometallic precursor species are introduced, the e-beam-deposited materials show nanocomposite structure with metal nano crystals of variable size embedded in an amorphous carbonaceous matrix. When precursor species used are only the residual hydrocarbon molecules issued from the pump oil, pure amorphous carbonaceous deposit is grown at the e-beam-treated locations (see Fig. 4).

In all cases, the growth rate of e-beam-deposited materials is strongly dependent on the vapor pressure in the chamber of the e-beam instrument, the e-beam parameters, the exposure time, and the substrate. The resolution of the EBID process is determined not only by the beam size of the primary electrons but also by the distribution of the secondary electrons and backscattered electrons emitted from the substrate. Thus, all reported measurements exhibit a broadening of the deposit compared to the beam diameter (see e.g. [26, 27]).

Due to the combination of high resolution and 3D structure formation, EBID is highly appreciated in the field of

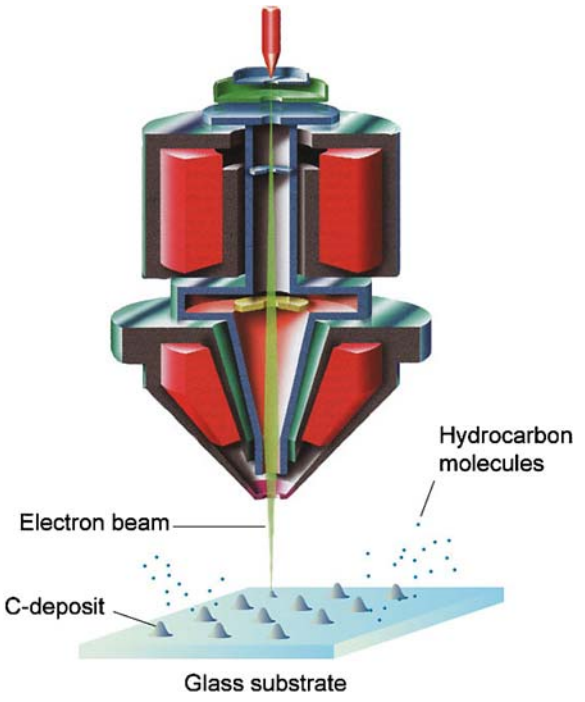


**Fig. 4** Principle of EBICD. The beam of electron cracks the residual hydrocarbon molecules issued from the pumping system leading to the formation of a solid carbonaceous deposit at the point of impact of the beam

exploratory nanodevice fabrication and has recently moved towards applications for production of conducting lines [28], X-ray mask repair [29], photonic crystals [30] and a wide range of devices [31–33]. Recently, it has been reported that e-beam-induced carbonaceous deposit can be used as a negative resist for electrochemical reactions i.e., it has been demonstrated that carbonaceous deposit in the nanometer range in thickness can block completely and selectively a wide range of chemical and electrochemical reactions even when it is exposed to extreme conditions —aggressive chemical environments and very high applied potentials—. According to the literature, e-beam-induced carbonaceous deposit is amorphous and consists mainly of a mixture of $sp^2$- and $sp^3$-bonded carbon [34]. The negative resist effect can be explained by the fact that carbonaceous nanostructures are not only chemically inert but also behave as an insulator. As a consequence, such type of nanomaterial can completely hamper subsequent chemical and electrochemical reactions.

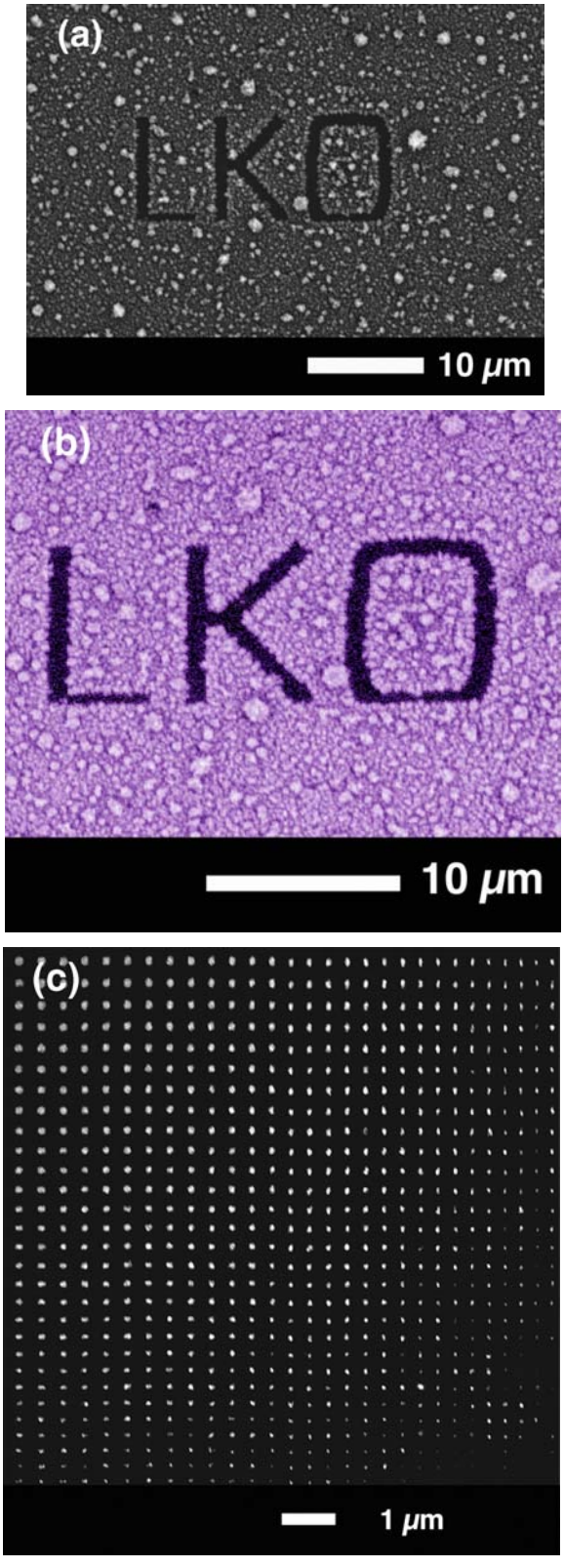


**Fig. 5** Nanomasking effect of e-beam-induced carbonaceous deposits for electroplating of metals performed under extreme conditions, (a) SEM image of *n*-type Si sample carrying a carbonaceous pattern "LKO" after a cathodic potentiodynamic experiment (from −0.1 to −1.0 V vs. (Ag/AgCl); sweep rate of 10 mV/s) performed in a 0.1 M $CuSO_4$ + 1 M $H_2SO_4$ electrolyte, (b) Corresponding AES mapping for Cu. (c) SEM micrograph of Au clusters showing sizes in the sub-50 nm range obtained by EBICD and electroplating of Au. Electrodeposition of Au was carried out by applying a potential step of −1.6 V (Ag/AgCl) for 10 s in a 10 mM $KAu(CN)_2$ + 1 M KC1 electrolyte. Reproduced by permission of the Electrochemical society, Inc

### 3.2. Micro- and nanostructuring by EBICD technique and electrodeposition

First, the high degree of selectivity achieved by e-beam-induced masking technique has been demonstrated for electrodeposition of Cu. Figure 5(a) shows a SEM image of *n*-type Si sample carrying a carbonaceous micropattern "LKO" written with a 1 C/cm$^2$ electron dose using a 20 keV beam energy after a cathodic potentiodynamic experiment (from −0.1 to −1.0 V vs. (Ag/AgCl); sweep rate of 10 mV/s) performed in a 0.1 M $CuSO_4$ + 1 M $H_2SO_4$ electrolyte. Clearly, the dark carbonaceous LKO micropattern surrounded by Cu crystallites corresponds to the masked area. Within this pattern, absolutely no deposited Cu particles could be detected even for very high cathodic potentials in acidic environment. The selectivity of the process due to the absence of Cu within the pattern has been confirmed by Auger Electron Spectroscopy (AES) mapping for Cu as it is shown in Fig. 5(b). More remarkably, it has been found that carbonaceous deposits in order of less than 1 nm thick can be sufficient to achieve a negative resist effect under different extreme conditions—high cathodic applied potentials in a cyanide environment, i.e. −1.6 V vs. (Ag/AgCl) for 10 s in 10 mM $KAu(CN)_2$ +1 M KCN—[35]. These results confirm the feasibility to exploit EBICD for the nanomasking of electrodeposition of metals on semiconductor surfaces. By optimizing e-beam parameters and electrodeposition conditions, electroplated Au clusters in the sub-50 nm range have been fabricated [36]. For this, a Si sample carrying two perpendicular arrays of carbonaceous lines (200 nm in width) with decreasing spacing were written with a 1 C/cm$^2$ electron dose using a 5 keV beam energy. Then, electrodeposition of Au was carried out by a potentiostatic experiment, i.e. high cathodic applied potential of −1.6 V (Ag/AgCl) for 10 s in a 10 mM $KAu(CN)_2$ + 1 M KCl electrolyte. Figure 5(c) shows that the features reveal a coherent formation of Au nanodots completely separated by the carbonaceous lines. The size of the dots decreases by decreasing the spacing between the carbonaceous lines. In this case, it has been reported that the beam energy as well as the applied potential are the predominant factors to achieve the fabrication of metallic nanostructures.

### 3.3. Microstructuring by EBICD technique and electrochemical etching

The masking effect of EBICD has also been demonstrated for the electrochemical etching of materials in extremely aggressive environment. Particularly, carbonaceous masking has been investigated to block the porosification of Si performed in HF electrolyte [37] as well as the corrosion of iron [38]. Figure 6(a) shows a SEM image of a *p*-type Si substrate carrying a rectangle carbonaceous micropattern (5 × 50 $\mu$m) written with a 3 mC/cm$^2$ electron dose after a galvanostatic experiment (anodic current of 0.1 A/cm$^2$ applied for 5 min) performed in a 20% HF electrolyte. Clearly, the masking effect is total as absolutely no sign of etching or dissolution is visible within the protected area. These results show the feasibility to exploit such carbonaceous deposit in extremely aggressive chemical environment for the porous Si micropatterning. Furthermore, photoluminescence measurements performed at different locations has revealed

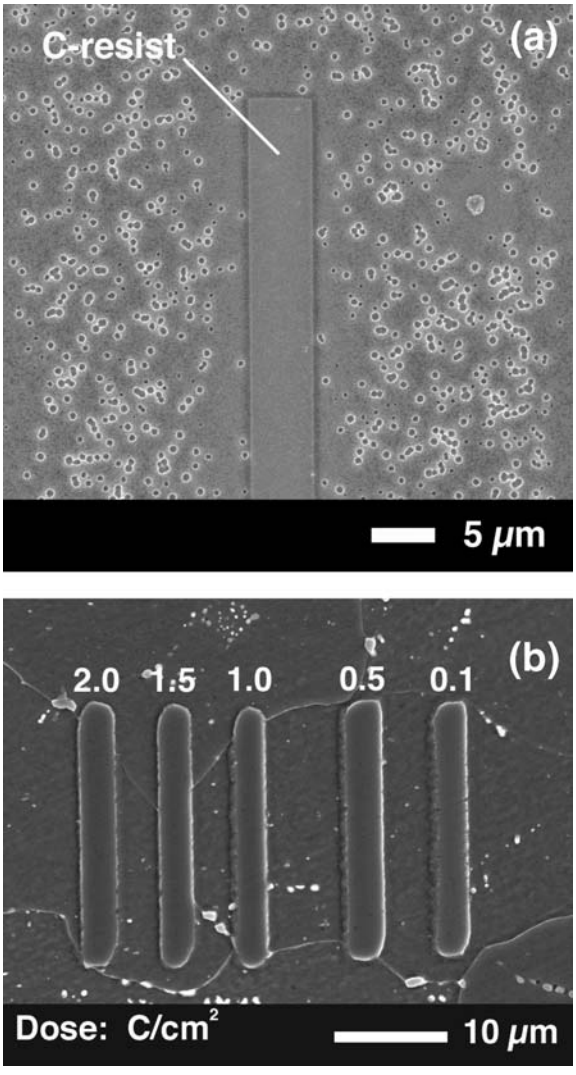


**Fig. 6** SEM images showing the high degree of protectiveness offered by the carbonaceous deposits, (a) Si sample carrying a rectangle carbonaceous pattern written with a 3 mC/cm$^2$ after galvanostatic experiment (0.1 A/cm$^2$ for 5 min) in 20% HF electrolyte. Reprinted from Surface Science, T. Djenizian, L. Santinacci, H. Hildebrand, and P. Schmuki, vol. 524, "Electron beam induced carbon deposition used as a negative resist for selective porous silicon formation" p. 40, 2003, with permission from Elsevier. (b) Carbonaceous patterned iron sample after a corrosion test by immersion in 3% $HNO_3$ for 2 min. Reproduced by permission of the Electrochemical society, Inc

a strong red visible luminescence (typical for porous Si) except for the carbonaceous treated locations suggesting that a high degree of selectivity can be achieved in view of optical properties. Figure 6(b) shows a SEM image of a carbonaceous micropatterned iron sample after a corrosion test by immersion in 3% $HNO_3$ for 2 min. Clearly, this chemical treatment leads to the selective dissolution of the iron surface resolving the grain structure of the substrate except at the e-beam treated locations. Furthermore, the high degree of protectiveness of EBICD has been also demonstrated for electrochemical corrosion experiments (see for example Ref. [38]).

## 4. Summary

The feasibility to combine e-beam writing approaches with different electrochemical treatments to fabricate structures in the sub-100 nm range is reported. The advantage of using conventional EBL with electroplating and electrochemical etching to fabricate high aspect ratios nanostructures is demonstrated.

In this overview, it is also reported that the blocking effect of e-beam-induced carbonaceous deposits for chemical and electrochemical reactions can be exploited to pattern various conductive substrates under extreme conditions. As e-beam-deposited nanomaterials remain still protective even in very harsh chemical environments and under extreme electrochemical conditions, this alternative e-beam writing approach opens new perspectives for micro- and nanostructuring surfaces as well as the micro- and nanomachining of a wide range of substrates.

**Acknowledgements** The authors thank the Deutsch-Franzosische Hochschule that supported the "First German-French Summer School on Electrochemistry and Nanotechnology" as well as the University of Erlangen-Nuremberg, the University of Provence, the CNRS, Metrohm, Autolab and Raith for their financial contributions.

TD acknowledges the assistance of Dr. A. Honsdorf from the Deutsch-Französische Hochschule.

## References

1. C.R. Friedrich, R. Warrington, W. Bacher, W. Bauer, P.J. Coane, J. Gottert, T. Hanemann, J. Hausselt, M. Heckele, R. Knitter, J. Mohr, V. Pioter, H.J. Ritzhaupt-Kleiss, and R. Ruprecht, in *Hanbook of Microlithography, Micromachining, and Microfabrication*, edited by P. Rai-Choudhury (SPIE Optical Engineering Press, Washington, 1997), vol. 2, p. 301.
2. Y. Xia, J.A. Rogers, K.E. Paul, and G.M. Whitesides, *Chem. Rev.,* **99**, 1823 (1999).
3. L. Stockman, I. Heyvaert, C. van Haesendonck, and Y. Bruynseraede, *Appl. Phys. Lett.*, **62**, 2935 (1993).
4. K. Matsumoto, M. Ishii, K. Segawa, Y. Oka, B.J. Vartanian, and J.S. Harris, *Appl. Phys. Lett.*, **68**, 34 (1996).
5. P.M. Campbell, E.S. Snow, and P.J. McMarr, *Appl. Phys. Lett.*, **66**, 1388 (1995).
6. P. Schmuki, S. Maupai, T. Djenizian, L. Santinacci, A. Spiegel, and U. Schlierf, *Encyclopedia of Nanoscience and Nanotechnology* (American Scientific Publishers, Stevenson Ranch, 2004), vol. 10, p. 393.
7. S. Borini, G. Amato, M. Rocchia, L. Boarino, and A.M. Rossi, *J. Appl. Phys.*, **93**, 4439 (2003).
8. K.C.A. Smith and C.W. Oatley, *Br. J. Appl. Phys.*, **6**, 391 (1955).
9. D.A. Buck and K. Shoulders, in Proceedings Eastern Joint Computer Conference, (ATEE, New York, 1957), p. 55.
10. A.N. Broers, *Microelectronics and Reliability*, **4**, 103 (1965).
11. A.N. Broers, W.W. Molzen, J.J. Cuomo, and N.D. Wittels, *Appl. Phys. Lett.*, **29**, 596 (1976).
12. D.R. Alice, C.P. Umbach, and A.N. Broers, *J. Vac. Sci. Technol. B*, **9**, 2838 (1991).
13. D.R. Alice and A. Broers, *Appl. Phys. Lett*, **57**, 2271 (1990).
14. S. Matsui, T. Ichihashi, and M. Mito, *Vac. Sci. Technol. B,* **7**, 1182 (1989).
15. X. Pan, D.R. Alice, A. Broers, Y.S. Tang, and C.W. Wilkinson, *Appl. Phys. Lett*, **59**, 3157 (1991).
16. H.G. Craighead, R.E. Howard, L.D. Jackel, and P.M. Mankiewich, *Appl. Phys. Lett*, **42**, 38 (1983).
17. A.N. Broers, *IBM J. Res. Dev.*, **32**, 502 (1988).
18. Gölzhäuser, W. Geyer, V. Stadler, W. Eck, M. Grunze, K. Edinger, T. Weimann, and P. Hinze, *J. Vac. Sci. Technol. B,* **18**, 3414 (2000).
19. M.J. Lercel, H.G. Craighead, A.N. Parikh, K. Seshadri, and D.L. Allara, *Appl. Phys. Lett*, **68**, 1504 (1996).
20. D.M. Eigler and E.I. Schweizer, *Nature*, **344**, 524 (1991).
21. C.P. Umbach, S. Washburn, R.B. Laibowitz, and R.A. Webb, *Phys. Rev. B,* **30**, 4048 (1984).
22. Muray, M. Scheinfein, M. Isaacson, and I. Adesida, *J. Vac. Sci. Technol. B*, **3**, 367 (1985).
23. G. Simon, A.M. Haghiri Gosnet, F. Carcenac, and H. Launois, *Microelectron. Eng.*, **35**, 51 (1997).
24. W. Xu, J. Wong, C.C. Cheng, R. Johnson, and A. Scherer, *J. Vac. Sci. Technol. B*, **13**, 2372 (1995).
25. A.P. Li, F. Miiller, and U. Gosele, *Electrochem. and Solid-State Lett.*, **3**, 131 (2000).
26. K.L. Lee and M. Hatzakis, *J. Vac. Sci. Technol. B*, **7**, 941 (1989).
27. K.T. Kohlmann von Platen, J. Chlebek, M. Weiss, K. Reimer, H. Oertel, and W.H. Brunger, *J. Vac. Sci. Technol. B*, **11**, 2219 (1993).
28. H.W.P. Koops, C. Schossler, A. Kaya, and M. Weber, *J. Vac. Sci. Technol. B*, **14**, 4105 (1996).
29. K.T. Kohlmann von Platen, M. Thiemann, and W. H. Brünger, *Microelectron. Eng.*, **13**, 279 (1991).
30. H.W.P. Koops, in *Photoreactive Fiber and Crystal Devices: Materials, Optical Properties, and Applications II*, edited by T.C. Hale and K. L. Telschow (Proceedings of SPIE, 1996), Vol. 2849, p. 248.
31. H.W.P. Koops, E. Munro, J. Rouse, J. Kretz, M. Rudolph, M. Weber, and G. Dahm, *Nucl. Instrum. Methods Phys. Res. B*, **363**, 1 (1995).
32. M. Weber, M. Rudolph, J. Kretz, and H.W.P. Koops, *J. Vac. Sci. Technol. B*, **13**, 461 (1995).
33. C. Schoessler and H.W.P. Koops, *J. Vac. Sci. Technol. B*, **16**, 862 (1998).
34. N. Miura, A. Yamada, and M. Konagai, *Jpn. J. Appl. Phys.*, **36**, L1275 (1997).
35. T. Djenizian, L. Santinacci, and P. Schmuki, *Appl. Phys. Lett.*, **78**, 2840 (2001).
36. T. Djenizian, L. Santinacci, and P. Schmuki, *J. Electrochem. Soc.*, **151**, G175 (2004).
37. T. Djenizian, L. Santinacci, H. Hildebrand, and P. Schmuki, *Surf. Sci.*, **524**, 40 (2003).
38. I. Sieber, H. Hildebrand, T. Djenizian, and P. Schmuki, *Electrochem. and Solid-State Lett.*, **6**, Cl (2003).